Oncogene (2020) 39:4103–4117
https://doi.org/10.1038/s41388-020-1260-1

ARTICLE

Hexosamine pathway inhibition overcomes pancreatic cancer resistance to gemcitabine through unfolded protein response and EGFR-Akt pathway modulation

Francesca Ricciardiello[1] · Yang Gang[2] · Roberta Palorini[1] · Quanxiao Li[2] · Marco Giampà[1] · Fangyu Zhao[2] · Lei You[2] · Barbara La Ferla[1] · Humberto De Vitto[1,4] · Wenfang Guan[3] · Jin Gu[3] · Taiping Zhang[2] · Yupei Zhao[2] · Ferdinando Chiaradonna[1]

Received: 12 October 2019 / Revised: 4 March 2020 / Accepted: 5 March 2020 / Published online: 31 March 2020

Abstract

Different evidence has indicated metabolic rewiring as a necessity for pancreatic cancer (PC) growth, invasion, and chemotherapy resistance. A relevant role has been assigned to glucose metabolism. In particular, an enhanced flux through the Hexosamine Biosynthetic Pathway (HBP) has been tightly linked to PC development. Here, we show that enhancement of the HBP, through the upregulation of the enzyme Phosphoacetylglucosamine Mutase 3 (PGM3), is associated with the onset of gemcitabine (GEM) resistance in PC. Indeed, mRNA profiles of GEM sensitive and resistant patient-derived tumor xenografts (PDXs) indicate that PGM3 expression is specifically increased in GEM-resistant PDXs. Of note, PGM3 results also overexpressed in human PC tissues as compared to paired adjacent normal tissues and its higher expression in PC patients is associated with worse median overall survival (OS). Strikingly, genetic or pharmacological PGM3 inhibition reduces PC cell growth, migration, invasion, in vivo tumor growth and enhances GEM sensitivity. Thus, combined treatment between a specific inhibitor of PGM3, named FR054, and GEM results in a potent reduction of xenograft tumor growth without any obvious side effects in normal tissues. Mechanistically, PGM3 inhibition, reducing protein glycosylation, causes a sustained Unfolded Protein Response (UPR), a significant attenuation of the pro-tumorigenic Epidermal Growth Factor Receptor (EGFR)-Akt axis, and finally cell death. In conclusion this study identifies the HBP as a metabolic pathway involved in GEM resistance and provides a strong rationale for a PC therapy addressing the combined treatment with the PGM3 inhibitor and GEM.

Introduction

Pancreatic cancer (PC) one of the most lethal types of cancer, is the fourth leading cause of cancer deaths in the USA [1], and will be the second leading cause of cancer deaths by 2030 [2]. Nearly 80% of patients are at an advanced stage and have lost an operation opportunity

These authors contributed equally: Francesca Ricciardiello, Yang Gang

Lead contact: Ferdinando Chiaradonna

Supplementary information The online version of this article (https://doi.org/10.1038/s41388-020-1260-1) contains supplementary material, which is available to authorized users.

✉ Taiping Zhang
tpingzhang@yahoo.com

✉ Yupei Zhao
zhao8028@263.net

✉ Ferdinando Chiaradonna
ferdinando.chiaradonna@unimib.it

[1] Department of Biotechnology and Biosciences, University of Milano-Bicocca, 20126 Milan, Italy

[2] Department of General Surgery, Peking Union Medical College Hospital, Chinese Academy of Medical Sciences and Peking Union Medical College, 100730 Beijing, China

[3] MOE Key Laboratory of Bioinformatics; Bioinformatics Division, Center for Synthetic and Systems Biology, BNRist; Department of Automation, Tsinghua University, 100084 Beijing, China

[4] Present address: Hormel Institute, University of Minnesota, Austin, MN 55912, USA

when diagnosed for lack of typical clinical symptoms in the early stage. Chemotherapy is the main treatment for these PC patients. Presently, monotherapy or combination treatment based on GEM is one of the most widely used schemes for PC [3]. However, these standard chemotherapies appear poorly effective in patients due to the development of resistance, which remains a significant clinical challenge and contributes to overall poor patient prognosis [4]. Exploring the mechanism of chemoresistance and finding new therapeutic targets for PC are of great significance for improving the prognosis of PC patients.

GEM-resistance has been associated with different mechanisms such as GEM transport and metabolism, tumor microenvironment and activation of survival signals (i.e., Epidermal Growth Factor Receptor (EGFR), Akt) [4, 5]. Furthermore, epithelial-to-mesenchymal transition (EMT) phenotype and cancer stem cells turn out to be also involved in chemoresistance [6]. Efficacy of GEM is also linked to its effect on cancer metabolism [7–9]. Of note, PC exhibits several metabolic alterations, including increased glucose and glutamine utilization and fatty acid synthesis [10]. Interestingly, a part of glucose, glutamine and Acetyl Coenzyme A are redirected in HBP and evidence indicate that increased flux through the HBP is necessary for PC cell survival, as well as for GEM resistance [7, 11–13]. This pathway, by sensing the availability of nutrients, couples metabolic flux to cell growth [13, 14] providing substrate for the *N*-glycosylation (*N*-gly) of plasma-membrane and secretory proteins and for the *O*-glycosylation (*O*-gly) of numerous nuclear and cytoplasmic proteins [13]. Consequently, the HBP has emerged as a regulator of several tumor features i.e., cell cycle [15], cell signaling and metabolism [16], stress response [17], and DNA damage repair [18]. Remarkably, oncogenic forms of KRAS, characterizing around 90% of PC, have been associated with increased levels of *N*-gly and *O*-gly [12, 19]. Given that GEM-resistance is due to multiple mechanisms, HBP inhibition, simultaneously targeting distinct features of tumor biology, could be really effective in avoiding drug resistance in PC tumor.

In this study, we investigated the effects of HBP inhibition by means of a novel inhibitor of the HBP's enzyme PGM3, FR054 [20, 21]. Our results indicate that GEM-resistance in PC is associated with enhancement of PGM3 expression and HBP flux that may cause a sustained activation of EGFR-Akt axis, this latter almost completely blunted by FR054. Therefore, our work reveals the rational for a combined therapy with the PGM3 inhibitor and GEM in PC patients.

Results

PGM3 is over-expressed in pancreatic GEM resistant PDX mice and in PC patients

To identify new molecular markers for GEM resistance, we treated 66 PC patient-derived tumor xenografts (PDXs) with GEM for 3 weeks and evaluated their response by measuring tumor growth inhibition rate (TGI%). According to the TGI%, PDXs were classified in four groups: top 25% for TGI as sensitive group ($n = 16$), PDXs between 25–50% as relative sensitive group ($n = 17$), PDXs between 50–75% as relative resistant group ($n = 17$), and the last 25% as resistant group ($n = 16$). Since we were interested in resistant PDXs as compared to sensitive ones, our further analyses were performed by considering only the sensitive and resistant groups in which the average TGI % was 125.7% and 33.7%, respectively (Fig. 1a). The PDXs' tumors in the sensitive group decreased significantly after GEM treatment, while GEM showed little effect on PDXs' tumors in the resistant group (Fig. S1). In order to clarify the molecular characteristics of drug-resistant and sensitive PDXs, we examined the messenger RNA (mRNA) profiles of PDX tumors from sensitive and resistant groups (data not shown). Among the differentially expressed genes between the two groups, the gene *PGM3/AGM1*, encoding for the HBP enzyme PGM3, was significantly upregulated in the resistant group (data not shown). Positive regulation in GEM resistant PDXs as compared to sensitive ones was confirmed by qPCR analysis of PGM3 mRNA (Fig. 1b). Then, we also analyzed the levels of PGM3 by immunohistochemistry (IHC) in 99 PC tissues from patients, showing that it was more highly expressed in the cancer tissues (Fig. 1c, d). In particular, in 66 patients who had both cancer and adjacent normal tissues, we also found a PGM3 score significantly higher in cancer tissues than paired adjacent normal ones (Fig. 1e). Most notably the Kaplan-Meier analysis revealed that PC patients with high PGM3 level ($n = 70$) had significantly worse median OS than those with low PGM3 level ($n = 25$) (10 vs. 43 months; $p = 0.012$; Fig. 1f). In addition, even though there was no significant correlation between PGM3 level and clinicopathological parameters (Table S1), univariate and multivariate analyses revealed that PGM3 level was negatively correlated with OS in both analyses, indicating that a high level of PGM3 is an independent prognostic risk factor for PC patients (Table S1).

To investigate in vitro whether GEM-resistance was related to PGM3 expression, we evaluated three different PC cell lines, BxPC-3, MIA PaCa-2 and PANC-1, for their GEM-sensitivity. Upon treatment with increasing

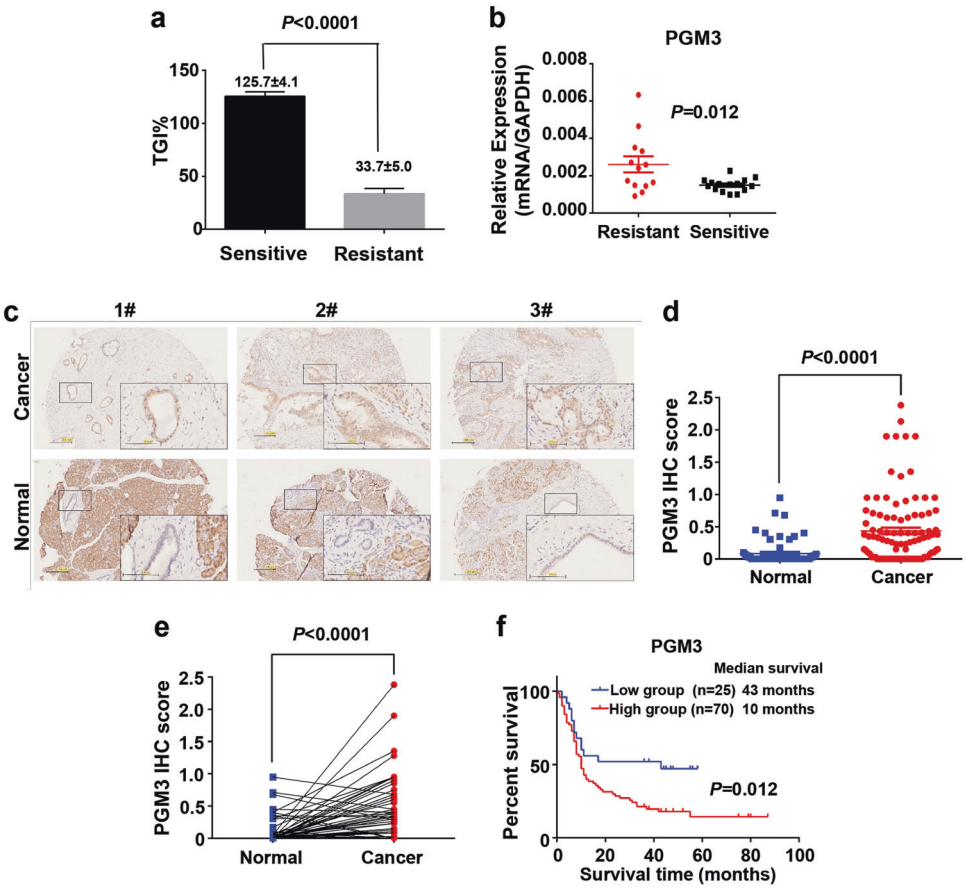

Fig. 1 PGM3 is upregulated in GEM resistant PDXs and negatively correlated with prognosis in PC. a TGI% of sensitive and resistant PDXs when treated with GEM. **b** mRNA expression of PGM3 in sensitive and resistant PDXs tissues. **c** Representative pictures of PGM3 in PC (up) and adjacent tissues (down). Magnification ×40, scale bars 200 µm. Enlarged areas are shown in boxes: magnification ×200, scale bars 100 µm. **d–e** IHC score of PGM3 in PC and adjacent tissues. **f** Kaplan-Meier survival analysis between high and low PGM3 level groups. Data are mean ± SEM. ***$p <$ 0.001 (T-student).

concentration of GEM, the three cell lines were analyzed in terms of proliferation (Fig. S2a, c) and death (Fig. S2b, d). BxPC-3 cells were the most sensitive while PANC-1 and MIA PaCa-2 cells were more resistant. Noteworthy is that the resistant cells MIA PaCa-2 and PANC-1 showed a significant basal higher expression of PGM3, mirroring the IHC analysis in PC patients, and of total protein *O*-gly as compared to BxPC-3 cells (Fig. S3a–c). In addition, analysis of PGM3 mRNA level (Fig. S3d, e), PGM3 protein level (Fig. S3f), as well as protein *O*-gly (Fig. S3f) upon increasing doses of GEM, indicated that PGM3 expression and protein *O*-gly are specifically enhanced in time-dependent and dose-dependent manner in resistant PANC-1 and MIA PaCa-2 cells, since, GEM sensitive BxPC-3 cells showed a completely opposite trend (Fig. S3g).

To further assess the association between GEM and PGM3 expression, we generated BxPC-3 and PANC-1 cells in which *PGM3* had been knocked out by short interfering RNA (siPGM3) or over-expressed (PGM3 OE) (Fig. S4a, b). The knocking out and the over-expression of PGM3 significantly increased and decreased, respectively, GEM sensitivity in both cell lines confirming that PGM3 plays a role in PC response to GEM treatment (Fig. 2a–d). These results agreed with the in vivo data (Fig. 1), indicating a positive correlation between PGM3 expression and GEM resistance.

PGM3 contributed to aggressive phenotype of PC cells by regulating proliferation, invasion, migration and mice tumor growth

Given that enhanced protein glycosylation in cancer has been associated with increased proliferation, EMT and metastasis [22], we used the recombinant BxPC-3 and PANC-1 cell lines (siPGM3 and PGM3 OE) to test the effect of changing PGM3 level on proliferation, migration and invasion. Reduction of PGM3 expression significantly decreased cell proliferation (Fig. 2e, f), invasion (Fig. 2g, h) and migration (Fig. 2j, k). Conversely, proliferation (Fig. S4c, d), invasion (Fig. S4e, f) and migration (Fig. S4g, h) were enhanced by PGM3 over-expression. To investigate the in vivo tumor function of PGM3, subcutaneous PC models were generated. Human BxPC-3 and MIA PaCa-2 cells stable expressing either scramble or *PGM3* short hairpin RNA (shRNA) were inoculated in SCID mice. The inoculation of the shPGM3 cells produced tumors that grew at a significantly slower rate either for BxPC-3 (Fig. 2i–m)

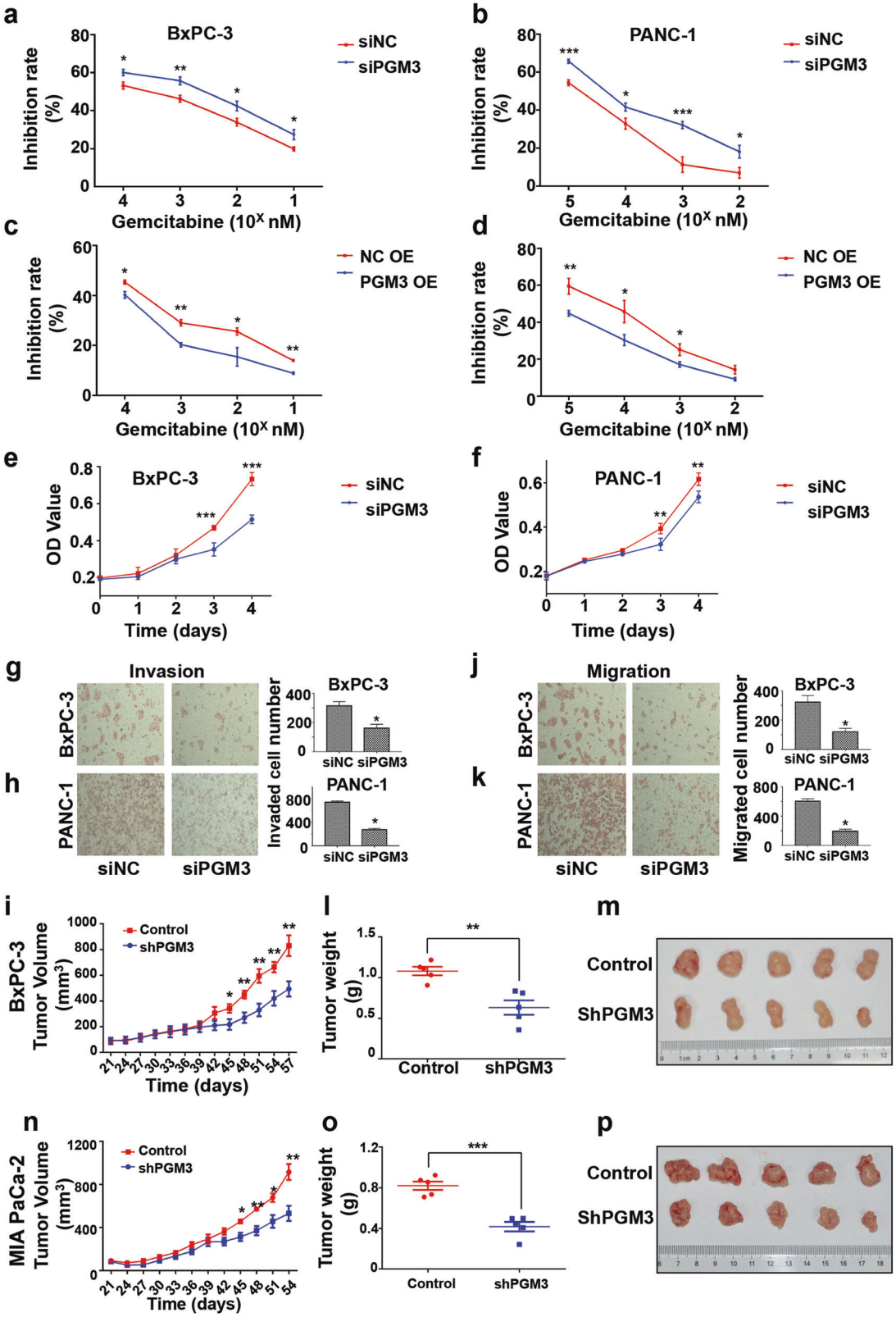

Fig. 2 PGM3 contributed proliferation, invasion, migration, chemoresistance in vitro and tumor growth in mice. a–b GEM sensitivity of siPGM3 BxPC-3 (**a**) and PANC-1 (**b**) cells. **c–d** GEM sensitivity of PGM3-OE BxPC-3 (**c**) and PANC-1 (**d**) cells. **e–f** Proliferation, (**g–h**) invasion and (**j–k**) migration of siPGM3 BxPC-3 and PANC-1 cells. **i–n** Tumor volume, (**l–o**) weight and (**m–p**) pictures of mice injected with shPGM3 or control BxPC-3 and PANC-1 cells. Data are mean ± SEM. $*p < 0.05$; $**p < 0.01$; $***p < 0.001$ (T-student).

or MIA PaCa-2 cells (Fig. 2n–p), revealing the involvement of PGM3 in PC in vivo growth as well.

PGM3 inhibitor FR054 enhances PC cell growth arrest and apoptosis

Since we have previously demonstrated the inhibitory effect of a novel compound, named FR054, on enzymatic activity of PGM3, as well as on proliferation of several breast cancer cells [20, 21], here, we decided to evaluate its effects also on GEM-sensitive and GEM-resistant PC cells. FR054 treatment, in concentration-dependent and time-dependent manner, reduced significantly cell proliferation (Fig. 3a–c), viability (Fig. 3d, e) and colony formation and size in all treated PC cell lines (Fig. 3f–h). To detail the cell death mechanism induced by FR054 treatment, we measured Annexin V (AV)-positive and Propidium Iodide (PI)-positive cells upon single or daily treatment with FR054. After 72 h treatment with 500μM FR054 the percentage of cell death (Fig. 3j, AV-positive and PI-positive cells) was similar to that shown in Fig. 3e. However, especially upon daily treatment, the cells were mostly AV-positive (Fig. 3k) and showed Caspase-3 activation (Fig. 3i–m) suggesting an apoptotic cell death mechanism. Importantly, FR054 treatment of non-tumoral human pancreatic ductal epithelial line (HPDE) induced cell growth arrest (Fig. S5a) without inducing cell death (Fig. S5b, c), excluding at least in this in vitro model, a toxic effect of FR054. Altogether these findings confirmed an important role of PGM3 in PC cells proliferation and survival.

FR054 treatment provides in vitro and in vivo enhanced GEM efficacy

Previous data indicate that PGM3 is involved in PC proliferation and GEM response, since its genetic or pharmacologically induced inhibition interferes with both processes. Therefore, we decided to evaluate if FR054 could enhance GEM efficacy in PC GEM-resistant cells, in resistant freshly isolated PDX derived tumor cells (PDTCs) and in GEM-resistant xenograft mice. As shown in Fig. 4a–d, combined treatment in MIA PaCa-2 and PANC-1 cell lines with 500 μM FR054 and 1 μM GEM (clinical dose) [23], yielded significantly greater growth inhibition and cell death than both agents alone. To further validate these results we also treated PDTCs from 17 different PDXs (all expressing an oncogenic form of KRAS) with different doses of the two drugs. Calculation of the half maximal inhibitory concentration (IC_{50}) of FR054 and GEM, ranging from 85.66 to 1467 μmol/L, and from 1.48×10^{-8} to 0.0179 μmol/L, respectively (Table S3), indicated a substantial variation of sensitivity between individual patient-derived models. Accordingly to the average IC_{50} of GEM and FR054, PDTCs were sorted into 5 resistant and 12 sensitive to GEM or FR054 (Table S3). Remarkably, the combined treatment between FR054 and GEM increased GEM-sensitivity in four of five GEM-resistant PDTCs (Fig. 4e and Table S3). Importantly, the correlation analysis showed that the IC_{50} of FR054 and GEM were positively related to the level of *PGM3* mRNA in PDTCs (Fig. S6a, b), and that the IC_{50} of FR054 was positively correlated with IC_{50} of GEM (Fig. S6c), suggesting that high *PGM3* level may lead to resistance to FR054 and GEM. These findings were further confirmed in treated xenograft mice. Indeed mice inoculated with GEM-resistant PANC-1 cells showed a significant tumor growth inhibition either under GEM and FR054 single treatments or upon combined treatment. In particular, the latter treatment appeared significantly stronger as compared to single ones (Fig. 4f–h). Moreover, treated mice did not lose weight (Fig. S7a) or show signs of kidney and liver toxicity (Fig. S7b, c) as compared to control and GEM treated mice. Conversely, serum analysis in combination therapy as compared to GEM alone, showed amelioration in some parameters (see Red Blood Cells (RBC) and Hemoglobin (Hb)) suggesting limited toxicity (Fig. S7d). Most notably, the combined treatment induced a stronger tumor growth inhibition also in GEM-resistant PDX mice -PDX-5- (Fig. 4j–i), further substantiating the efficacy of FR054 as an adjuvant therapy in PC cells and tumor treated with GEM.

PGM3 inhibition alone and in combination with GEM induces a sustained activation of the pro-apoptotic UPR protein Chop in resistant PC cells

Based on our previous findings demonstrating that the inhibition FR054-dependent of PGM3 caused a reduction of protein *N*-gly and *O*-gly and activation of the UPR [21], we decided to evaluate both effects also in PC cells. Confocal microscopy or flow cytometric analysis by using the lectin *Phaseolus vulgaris* (PHA-L), able to recognize membrane tri-/tetra-antennary structures, showed a significant decrease of PHA-L reactivity in all PC cells upon 48 h of FR054 treatment (Fig. 5a–c). In addition, more prolonged treatment with FR054 (72 h) reduced also *O*-gly in both MIA PaCa-2 and BxPC-3 cells and induced a clear change in the *O*-gly protein pattern of PANC-1 cells, validating the inhibitory effect of FR054 on HBP (Fig. S8a). In association with the membrane protein *N*-gly reduction, PC cells, despite a different temporal trend, modulate mRNAs, such as *DDIT3/CHOP*, *XBP1*, *ATF4,* and *HSPA5* (Fig. 5d), and proteins, such as ATF4, phosphorylated elongation factor 2α (p-elF2α) and Chop (Fig. 5e), tightly associated to UPR activation. Notably, Chop protein, an important transcription factor associated with the UPR-induced apoptosis, was

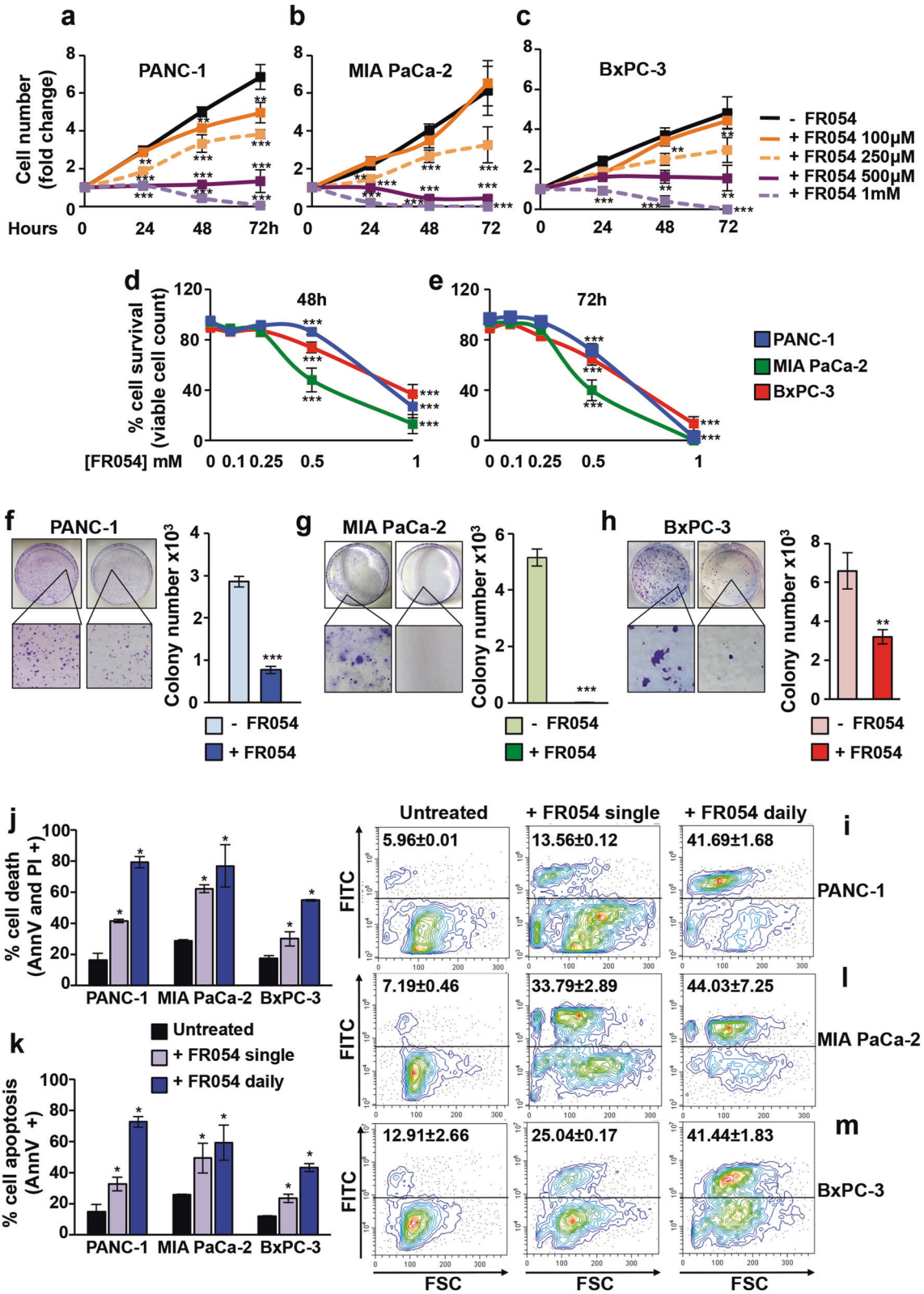

Fig. 3 Targeting PGM3 induces cell growth arrest and apoptosis. **a–c** Cell number and (**d–e**) cell survival of PANC-1, MIA PaCa-2, and BxPC-3 cells upon different doses of FR054. **f–h** Representative images of cell colony assay upon single treatment with vehicle (medium) or 500 µm FR054. Quantization of (**j**) AV/PI positive cells, (**k**) AV positive cells and (**i–m**) Caspase-3 activation upon 48 h of single or daily FR054 treatment. Data are mean ± SEM. $*p < 0.05$; $**p < 0.01$; $***p < 0.001$ (T-student).

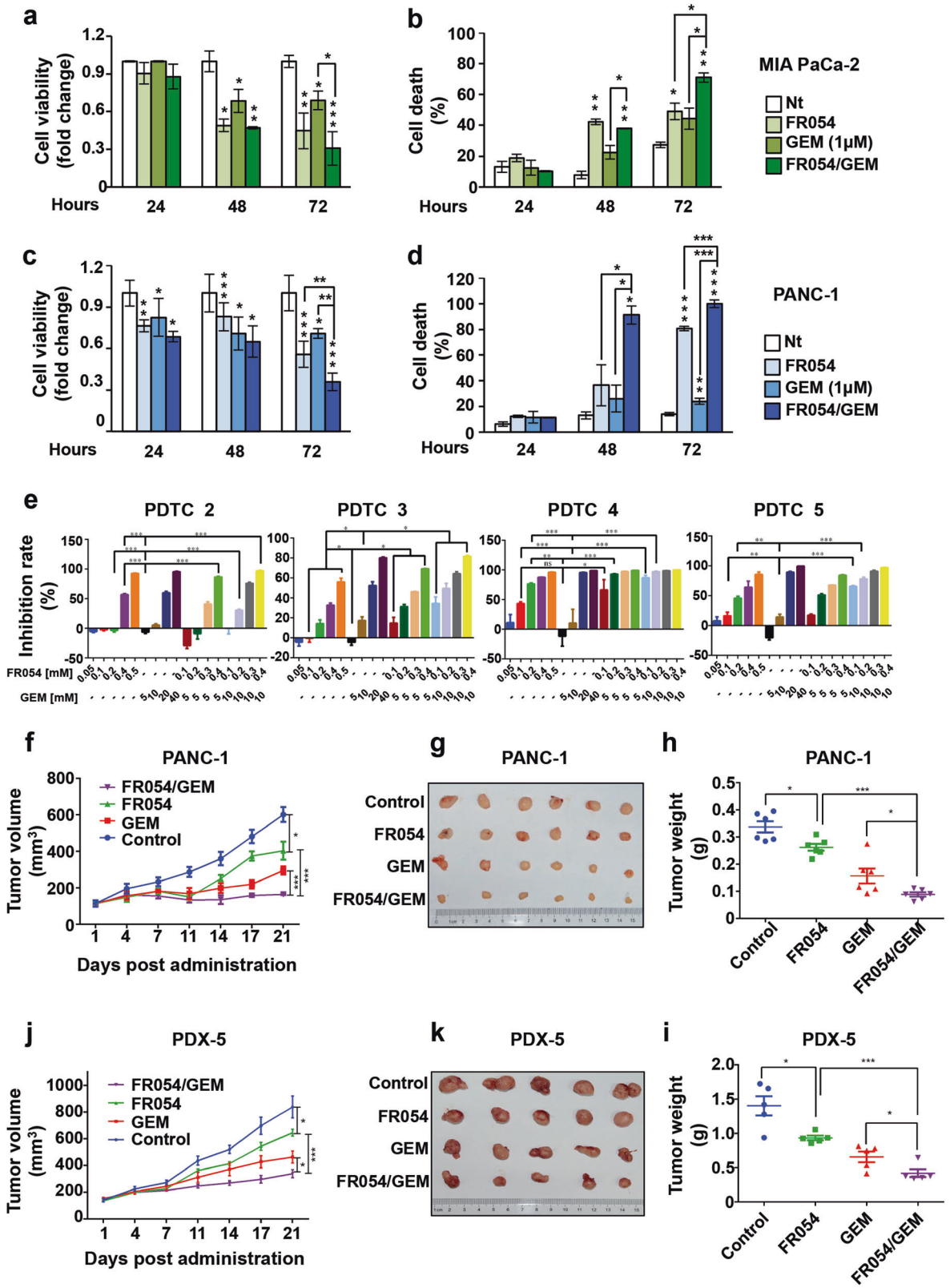

Fig. 4 FR054 synergizes with GEM and suppresses in vitro and in vivo proliferation. (**a**–**c**) Cell viability and (**b**–**d**) death of MIA PaCa-2 and PANC-1 cells upon single treatment with FR054 and GEM alone or their combination (24, 48 and 72 h). **e** Proliferation of PDTCs treated with FR054 and GEM alone or their combination (48 h). **f** and **j** Tumor volume, (**g** and **k**) image and (**h** and **i**) weight of PANC-1 and PDX-injected mice upon treatment with FR054 and GEM alone or their combination, respectively. Data are mean ± SEM. $*p < 0.05$; $**p < 0.01$; $***p < 0.001$ (T-student).

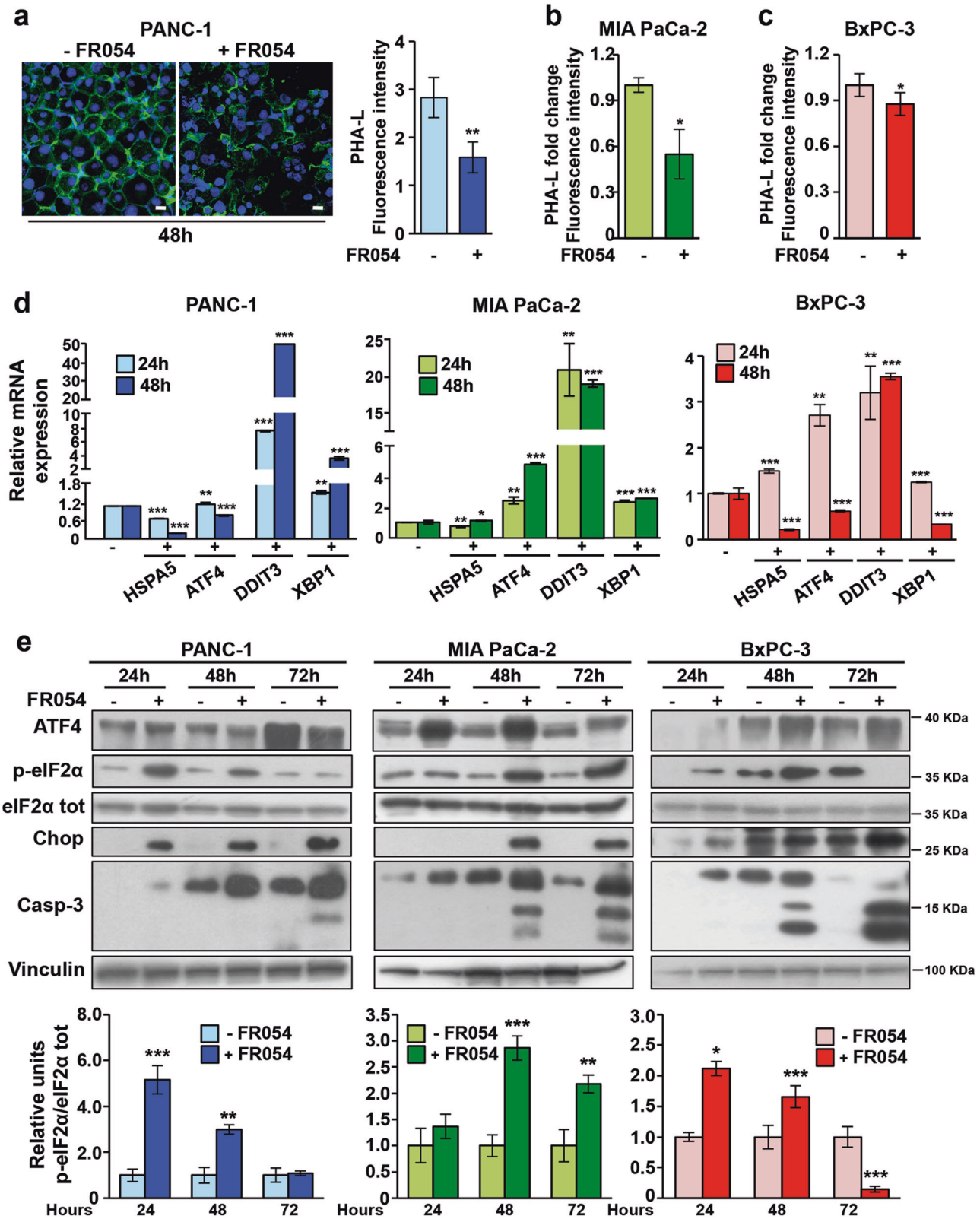

Fig. 5 FR054 induces a sustained activation of UPR. a Confocal microscopy (magnification ×40, scale bar 20 µm) and (**b**–**c**) FACS analysis of PHA-L staining in PANC-1, MIA PaCa-2, and BxPC-3 cells treated for 48 h with FR054. **d** mRNA expression in PC cells following 24 h and 48 h FR054 treatment. **e** Representative western blots and band quantization of UPR proteins. Data are mean ± SEM. $*p < 0.05$; $**p < 0.01$; $***p < 0.001$ (T-student).

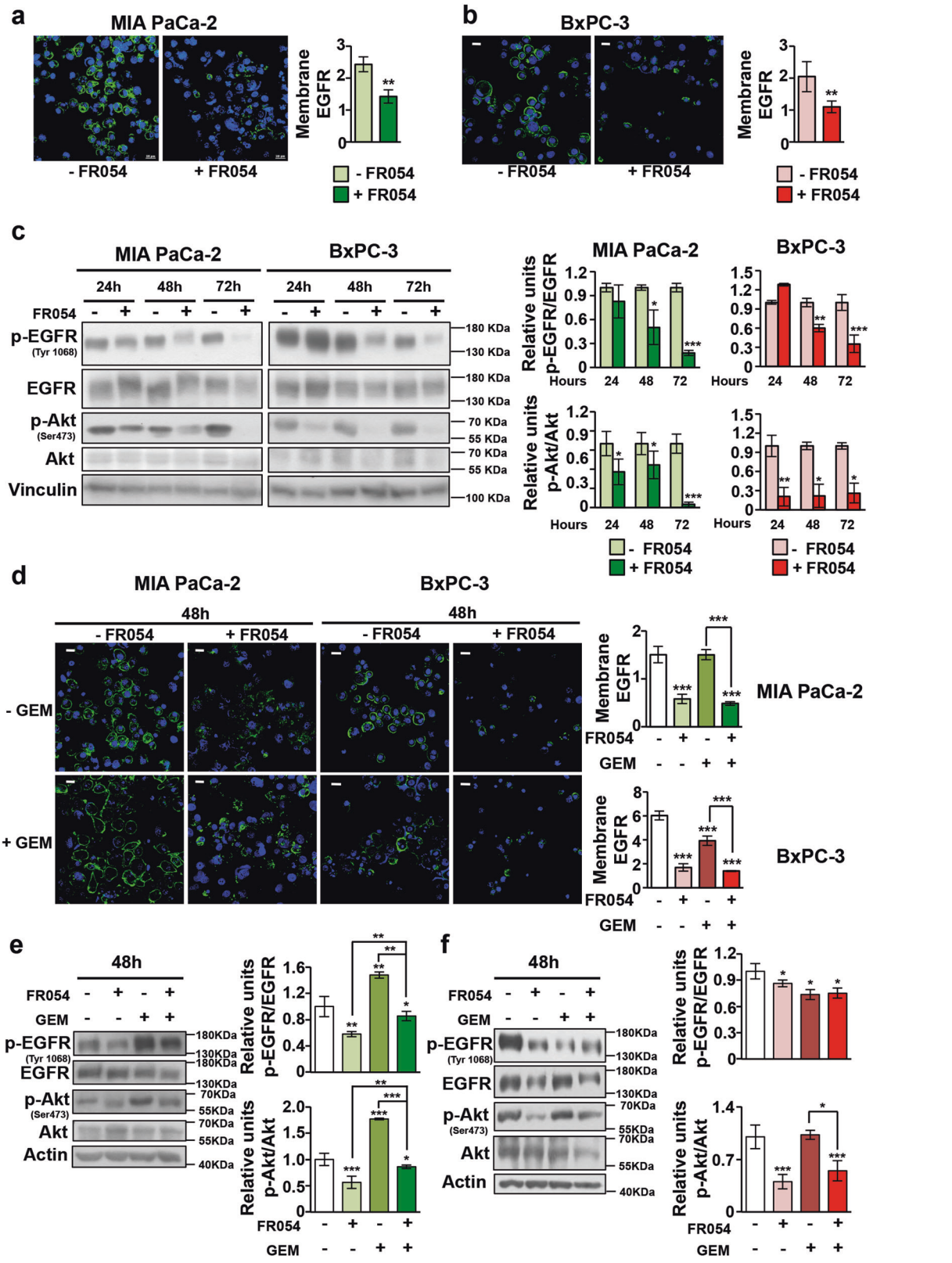

highly expressed (Fig. 5e), nuclear localized (Fig. S8b) and with a trend of expression comparable to Caspase-3 cleavage (Fig. 5e) particularly in FR054 treated samples, suggesting that pharmacological PGM3 inhibition, causing a decrease in protein glycosylation, leads to UPR activation and finally to cell death.

◀ **Fig. 6 FR054 inhibits EGFR-Akt axis.** Confocal microscopy analysis of membrane EGFR staining in (**a**) MIA PaCa-2 and (**b**) BxPC-3 cells treated with FR054 for 48 h (magnification ×40, scale bar 25 µm). **c** Protein expression and band quantization for p-EGFR and p-Akt in MIA PaCa-2 and BxPC-3 upon FR054 treatment. **d** Confocal microscopy analysis of membrane EGFR staining in MIA PaCa-2 and BxPC-3 upon treatment with FR054 and GEM alone or their combination (magnification ×40, scale bar 25 µm). Protein expression and band quantization for p-EGFR and p-Akt in (**e**) MIA PaCa-2 and (**f**) BxPC-3 upon treatment with FR054 and GEM alone or their combination. Data are mean ± SEM. $*p < 0.05$; $**p < 0.01$; $***p < 0.001$ (T-student).

ER stress and UPR are upregulated in many cancers, thus presenting the possibility of an association with drug-resistance [reviewed in [24]] and specifically GEM-resistance [25]. Therefore, we examined UPR activation upon single or combined treatment in PANC-1, MIA PaCa-2, and BxPC-3 cells, with a focus on the Chop protein whose increased level of expression may shift the function of the UPR from pro-survival, i.e., under drug treatment, to pro-apoptotic [25, 26]. As shown in Fig. S8c, d, in GEM-resistant cells PANC-1 and MIA PaCa-2, Chop expression increased at a significantly higher level in single or combined FR054 treated samples as compared to GEM alone. Conversely, in GEM-sensitive BxPC-3 cells, Chop increased in all treated samples but in particular in the GEM alone treated sample. Having established that further experiments are required in order to understand better the relation between GEM-sensitivity and UPR activation, altogether these data suggest that a strong UPR activation induces PC cell death, increasing GEM sensitivity, and that the greater sensitivity of BxPC-3 cells may be also the consequence of the GEM-dependent activation of the UPR pro-apoptotic protein Chop.

FR054 alone or in combination with GEM downregulates the EGFR membrane localization and activity in PC cells and xenograft tumors

Our previous data indicated that FR054 induces a significant reduction of tri/tetra antennary *N*-gly membrane proteins; thus, it could impact on signaling necessary to tumor survival and proliferation. Among the different receptors, EGFR has been described as essential to PC initiation, maintenance, aggressiveness and cancer resistance to therapy [27]. In addition, EGFR activation and localization is controlled by its glycosylation state [28, 29]. By using an antibody recognizing the EGFR extracellular domain, we demonstrated that EGFR membrane localization was significantly reduced after FR054 treatment (Fig. 6a, b). Since membrane localization is associated to catalytic activity of EGFR and activation of downstream signaling pathways, we evaluated the phosphorylation of EGFR tyrosine 1068 and of Akt serine 473. Both significantly decreased upon FR054 treatment (Fig. 6c). To determine if GEM and/or FR054 sensitivity were associated to EGFR signaling activation, we evaluated EGFR signaling under single and combined treatments in PC cells. As shown in MIA PaCa-2 cells, GEM treatment significantly activated both EGFR and Akt without changing EGFR membrane localization (Fig. 6d, e). Strikingly, FR054 significantly inhibited the positive effect of GEM on EGFR signaling, as it induced a reduction in membrane localization and EGFR and Akt activation as compared to GEM alone (Fig. 6d, e). Noteworthy is the fact that also in GEM-resistant PANC-1 cells, EGFR membrane localization was induced by GEM and drastically reduced by FR054 alone or in combination (Fig. S9a), further suggesting that PGM3 inhibition could restore GEM sensitivity by down-regulation of EGFR activity. This hypothesis was corroborated by analysis of EGFR signaling in sensitive BxPC-3 cells. Indeed, upon GEM treatment, a reduction of EGFR membrane localization and a significant decrease in EGFR and Akt phosphorylation were observed, effects that were further increased by FR054 co-treatment (Fig. 6d, f). Altogether these findings pointed out EGFR signaling inhibition as a key event in producing GEM cytotoxicity. Taking in consideration that almost 10% of PC patients show a wild type form of KRAS, we decided to test if FR054 could improve GEM efficacy also in KRAS wild type cell line BxPC-3. As expected from previous findings, a significant reduction in cell survival was observed in combined treatment as compared to single ones (Fig. S9b), and hence suggesting that enhancement of HBP is associated to PC survival under normal and stress conditions i.e., GEM treatment.

Our in vitro findings indicated that combined treatment could be effective against PC by upregulating the pro-apoptotic protein Chop and downregulating EGFR signaling. To determine whether these mechanisms of drug action were observed also in vivo, tissues from PANC-1 and PDX-5 sacrificed mice treated with single drugs or their combination, were used to evaluate the effect of FR054 and GEM either alone or in combination by IHC. Figure 7a, b show that Chop and Caspase-3 are highly expressed in the FR054 treated groups. Conversely, the same tissues show an opposite trend for Ki67 (proliferative marker), EGFR phosphorylation and PGM3. Most notably, EGFR phosphorylation level and PGM3 expression are both enhanced in GEM treated samples (Fig. 7a, b) and almost completely inhibited by FR054 co-treatment, mirroring the previous in vitro data. Collectively, the results from the mouse models reveal that the activation of UPR and the inhibition of EGFR signaling could explain the efficacy of combining GEM and FR054 against PC.

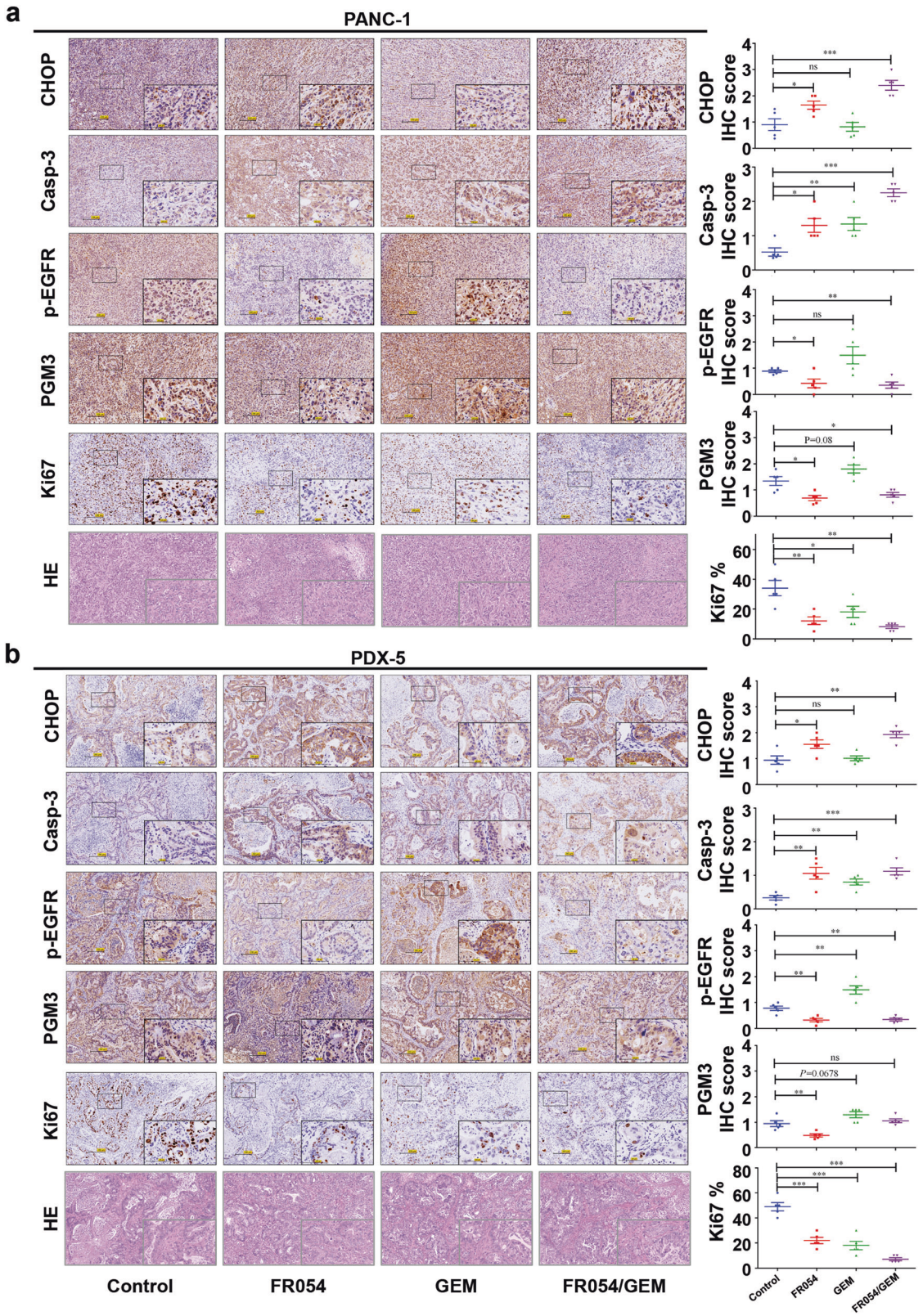

Fig. 7 IHC and HE staining of PANC-1 and PDX-5 xenograft tumors. a–b Representative pictures (left) of the IHC of Chop, Casp-3, p-EGFR, PGM3, Ki67, their HE staining and IHC score (right) of PANC-1 xenograft (**a**) and PDX-5 (**b**) tumors. Magnification ×40, scale bar 200 µm. Enlarged areas are shown in boxes: magnification ×200, scale bar 100 µm. Data are mean ± SEM. *$p < 0.05$; **$p < 0.01$; ***$p < 0.001$ (T-student).

Discussion

Although GEM remains the most used chemotherapeutic drug in PC, it has a low response since a rapid development of resistance often follows the initial sensitivity in patients. New therapies exploiting synergism with GEM are addressed either to more aggressive regimens (i.e., GEM plus Nab-paclitaxel) or to inhibition of some resistance mechanisms [3, 30, 31]. To note, accumulating evidence indicates that also cancer metabolic alterations influence GEM resistance in PC [7–9, 32].

Here, we reveal an important metabolic mechanism underlying GEM-resistance in PC. Indeed, we identify that PC GEM-resistant PDX mice and cell lines upregulate *PGM3* expression, a key enzyme of HBP. Noteworthy is that PGM3 and HBP levels increase only in GEM-resistant PC cells since sensitive ones show a completely opposite trend, suggesting a causative correlation between GEM-resistance and PGM3 expression. This causative role is further suggested by the positive relation between the IC_{50} of GEM and the *PGM3* mRNA level and by the individuation of PGM3 as unfavorable prognosis marker in our patient cohort. Notably, PGM3 has been identified as an unfavorable prognostic marker also in renal, cervical and breast cancer [33]. Association between PC growth and HBP activation has been already observed upon hypoxia or oncogenic KRAS activation [11, 12]. In both cases, accordingly to our results, direct inhibition of HBP pathway causes a decrease in cell proliferation and survival.

From a mechanistic point of view, an increased flux through HBP, achieved by enhancing of PGM3, may represent an efficient mechanism to induce a multifactorial response such as GEM-resistance. Indeed, different findings revealed that an enhancement of HBP flux concurrently influences several aspects of tumor biology. For instance, increased expression of the HBP's enzyme Glucosamine fructose-6-phosphate aminotransferase 1 (GFAT1) or protein *O*-gly positively controls proliferation, migration and chemoresistance by increasing for example the stability and activity of different oncogenes [34–37]. Accordingly, here, we demonstrate that GEM-resistant tumor and PC cells, in contrast to the sensitive models, show higher levels of PGM3 and *O*-gly either at basal state or under GEM treatment. The important role of PGM3 in PC growth and GEM-resistance is also well documented by the experiments with PGM3 silenced and over-expressed in which a direct role of PGM3 in proliferation, migration, invasion, tumor growth in mice and GEM-resistance is shown.

Mechanistically, we show that chemical inhibition of PGM3 alone or in combination with GEM treatment favors a pro-apoptotic UPR activation associated with a strong inhibition of EGFR signaling. Importantly, recent evidence suggests that drugs enhancing ER stress cause PC cell death [38] and modulate the chemosensitivity [25, 39, 40]. Accordingly, our experiments show that resistant and sensitive cells have a completely opposite behavior regarding UPR modulation upon GEM treatment, suggesting that UPR activation, i.e., by inhibiting PGM3, may be an effective approach to overcome GEM-resistance. Regarding EGFR, enhanced activity has been already associated to GEM resistance in PC [41], indeed new therapies exploiting synergy between GEM and EGFR inhibition are an important ongoing clinical effort. Besides, our in vitro and in vivo data suggest that the opposite EGFR response to GEM in sensitive and resistant cells is a key determinant for GEM-resistance. Indeed, FR054-dependent attenuation of EGFR activation is tightly linked to its ability to enhance GEM sensitivity in resistant cells or mice. However, the ability of FR054 to reduce PC cell growth independently from GEM sensitivity further substantiates PGM3 inhibition as a therapeutic approach.

In conclusion, while we recognize that the mechanism of action of FR054 in PC deserves further studies, we believe that therapeutic approaches involving PGM3 inhibition in combination with GEM require immediate clinical investigation for this deadly tumor.

Materials and methods

Cell lines

Human PC cell lines PANC-1 and MIA PaCa-2 and BxPC-3 were routinely cultured in high glucose Dulbecco's modified Eagle's medium (DMEM) and RPMI, respectively, supplemented with 2 mM L-glutamine, 100 U/mL penicillin, 100 mg/mL streptomycin and 10% fetal bovine serum. All cell lines were purchased from the American Type Culture Collection (ATCC) and tested for mycoplasm every two months.

The normal human pancreatic duct epithelial (HPDE) cells were routinely cultured in Keratinocyte-SFM medium, supplemented with 2 mM L-glutamine, human recombinant Epidermal Growth Factor 1–53 (EGF 1–53), Bovine Pituitary Extract (BPE), 100 U/mL penicillin, 100 mg/mL streptomycin.

siPGM3 and PGM3 overexpressed cell lines

siRNA targeting PGM3 and a scramble control siRNA were purchased from Guangzhou RiboBio Co., LTD. (Guangzhou, China). A full length PGM3 cDNA (NM_001199917.2) was fused into a pcDNA 3.1 empty vector to generate pcDNA3.1-PGM3 expression construct. See Supplementary material for details.

Clinical specimens

The clinical pancreatic cancer specimens were obtained from patients who received surgery in the Peking Union Medical College Hospital and employed for the construction of a tissue microarray (TMA) and PDXs models. The clinical and pathologic data of patients were obtained from the same hospital. All patients were provided informed consent for the tumor samples. The program was approved by the Ethics Committee of Peking Union Medical College Hospital.

Generation and resuscitation of pancreatic cancer PDX models

The generation and resuscitation of pancreatic cancer PDX models were conducted as described previously [42]. See Supplementary material for details.

The treatment of pancreatic cancer models

All animal experiments were performed according to the institutional ethical guidelines of Peking Union Medical College. Mice were in specific pathogen free (SPF) condition. For GEM treatment on PDX models, twelve PDXs models were randomly divided into two groups, 6 mice in each group when the volume of the tumor reaches 100–300 mm^3. One group is administrated by GEM, 60 mg/kg, IP, Q4D*6 for three weeks, and the other group was treated with physiological saline at the same way. The behavior of animals was monitored every day after administration. The calculation of tumor growth inhibition rate (TGI%) is described in Supplementary material. For FR054 and GEM combined treatment, the subcutaneous xenograft tumor mouse models of PANC-1 or PDXs were constructed. See Supplementary material for details.

Xenograft tumor mouse models

5×10^6 PC cells with PGM3 stably knocked down or the control cells were injected subcutaneously into 5 mice for group. The tumor volume was measured by vernier calipers and the mice were weighed every three days. Tumor volume was calculated using the formula $(a \times b \times b)/2$, where a and b are the major and the minor tumor axis, respectively. The mice were sacrificed after two months. The tumors were separated and weighed.

The isolation, propagation, and treatment on PDTCs

Conditional reprogram methods to get PDTC, as previously published [43], have been used. Feeder cells were plated into 96-well plate at 3×10^4/well. Single cell suspension from PDXs was inoculated into the 96-well plate containing feeder cells at 2000–5000/well. Cell plates were cultured in a 5% CO_2 incubator at 37 °C. After 24 h, GEM or FR054 with proper concentration was added into the 96-well plate, and the cells were counted by Edu method. Feeder cells and Edu (RUO-00501#1T and RUO-00401#150T, Beijing Zhikangbo Pharmaceutical Oncology Medical Research Co,.Ltd. China) according to the manufacturer's protocol after 48 h. See Supplementary material for more details.

Cell treatment and cell viability and proliferation evaluation

Where not differently specified, all the experiments with the cells were performed after seeding in growth medium followed by further 24 h before GEM and FR054 treatments. GEM was purchased from Sigma-Aldrich. FR054 was synthesized either by our laboratories [20, 21] or by WuXi AppTec Co., Ltd (Tianjin, China). For siPGM3 and PGM3oe cell lines, Cell Counting Kit-8 (CCK-8) reagent (Dojindo, Tokyo, Japan) was used to perform growth assays following the manufacturer's protocol.

See Supplemental methods for details.

Cell migration and invasion assays

Cell migration and Matrigel cell invasion assays were conducted as described previously [44]. See Supplementary material for details.

Western blot analysis

25 to 50 μg of total protein were resolved by SDS-PAGE, transferred to the nitrocellulose membrane and incubated overnight with specific antibodies. See Supplementary material for details.

Confocal microscopy analyses

For detection of cell surface expression of *N*-linked glycoproteins and of membrane EGFR, cells were stained with PHA-L and membrane EGFR antibody (against the extracellular domain of human EGFR), respectively. See Supplementary material for details.

RNA extraction and semiquantitative RT-PCR analysis

See Supplementary material for details.

Flow cytometric analysis

All flow cytometric analyses were performed using the flow cytometer CytoFLEX, Beckman Coulter. Both the

acquisition and the analysis of the data were performed with the CytExpert Software. See Supplementary material for details.

Immunohistochemistry analysis

PGM3 (H00005238-M01, Abnova, Taiwan, China) antibody was used to measure PGM3 expression in TMA by IHC as previously described [45]. The adjacent cancer tissue per PC patient verified by pathology were defined as Normal. See Supplementary material for details.

Statistics

For experiments with cell lines, unless otherwise noted, all results are presented as mean ± SEM and as mean ± SD from three or more independent experiments and statistical significance ($*p < 0.05$, $**p < 0.01$, $***p < 0.001$) is determined using Student's *t*-test.

For mice experiments, each experiment was repeated at least three times. Data were measured by Student's *t*-test (two-tailed) and analyzed using one-way ANOVA. All statistical tests were performed using the Statistical Program for Social Sciences (SPSS16.0 for Windows, USA) and were two-sided. *P* value of <0.05 was regarded as statistically significant. IC50 of FR054 in PDTCs was calculated by Nonlinear regression using Graphpad Prism 6.0 for windows (USA). Correlation between PGM3 expression and clinical parameters was calculated by Pearson chi-square tests. Risk factors for pancreatic cancer patients have been calculated by COX-regression analysis.

Acknowledgements FC was supported by grants from MAECI (Executive Programme of Scientific and Technological Cooperation Italy-China 2019–2021, #CN19GR03), from Associazione Italiana per la Ricerca sul Cancro (A.I.R.C., IG2014 Id.15364) and Fondo individuale FFABBR_NAT 2017 (MIUR, Italy). TZ was supported by grants from Key Projects of International Scientific and Technological Innovation Cooperation Between Chinese and Italian Governments (2018YFE0118600), from the National Natural Science Foundation of China (No. 81772639), from Natural Science Foundation of Beijing (No. 7192157) and CAMS Innovation Fund for Medical Sciences (CIFMS) (No. 2016-I2M-1-001). YZ was supported by grants from Non-profit Central Research Institute Fund of Chinese Academy of Medical Sciences (No. 2018PT32014). FR is supported by fellowship from MIUR. RP and HDV were supported by fellowship from MIUR and National Brazilian Institution of Science (CAPES 9281-13-4), respectively. We thank Neil Campbell for English editing.

Compliance with ethical standards

Conflict of interest The authors declare that they have no conflict of interest.

Publisher's note Springer Nature remains neutral with regard to jurisdictional claims in published maps and institutional affiliations.

References

1. Siegel RL, Miller KD, Jemal A. Cancer statistics, 2019. CA Cancer J Clin. 2019;69:7–34.
2. Rahib L, Smith BD, Aizenberg R, Rosenzweig AB, Fleshman JM, Matrisian LM. Projecting cancer incidence and deaths to 2030: the unexpected burden of thyroid, liver, and pancreas cancers in the United States. Cancer Res. 2014;74:2913–21.
3. Binenbaum Y, Na'ara S, Gil Z. Gemcitabine resistance in pancreatic ductal adenocarcinoma. Drug Resist Updat. 2015;23:55–68.
4. Amrutkar M, Gladhaug IP. Pancreatic cancer chemoresistance to gemcitabine. Cancers. 2017;9:157.
5. de Sousa Cavalcante L, Monteiro G. Gemcitabine: metabolism and molecular mechanisms of action, sensitivity and chemoresistance in pancreatic cancer. Eur J Pharm. 2014;741:8–16.
6. Luo W, Yang G, Qiu J, Luan J, Zhang Y, You L, et al. Novel discoveries targeting gemcitabine-based chemoresistance and new therapies in pancreatic cancer: How far are we from the destination? Cancer Med. 2019;8:6403–13.
7. Chen R, Lai LA, Sullivan Y, Wong M, Wang L, Riddell J, et al. Disrupting glutamine metabolic pathways to sensitize gemcitabine-resistant pancreatic cancer. Sci Rep. 2017;7:7950.
8. Shukla SK, Purohit V, Mehla K, Gunda V, Chaika NV, Vernucci E, et al. MUC1 and HIF-1alpha signaling crosstalk induces anabolic glucose metabolism to impart gemcitabine resistance to pancreatic cancer. Cancer Cell. 2017;32:392.
9. Tadros S, Shukla SK, King RJ, Gunda V, Vernucci E, Abrego J, et al. De novo lipid synthesis facilitates gemcitabine resistance through endoplasmic reticulum stress in pancreatic cancer. Cancer Res. 2017;77:5503–17.
10. Vaziri-Gohar A, Zarei M, Brody JR, Winter JM. Metabolic dependencies in pancreatic cancer. Front Oncol. 2018;8:617.
11. Guillaumond F, Leca J, Olivares O, Lavaut MN, Vidal N, Berthezene P, et al. Strengthened glycolysis under hypoxia supports tumor symbiosis and hexosamine biosynthesis in pancreatic adenocarcinoma. Proc Natl Acad Sci USA. 2013;110:3919–24.
12. Ying H, Kimmelman AC, Lyssiotis CA, Hua S, Chu GC, Fletcher-Sananikone E, et al. Oncogenic Kras maintains pancreatic tumors through regulation of anabolic glucose metabolism. Cell. 2012;149:656–70.
13. Chiaradonna F, Ricciardiello F, Palorini R. The Nutrient-sensing hexosamine biosynthetic pathway as the hub of cancer metabolic rewiring. Cells. 2018;7:E53.
14. Akella NM, Ciraku L, Reginato MJ. Fueling the fire: emerging role of the hexosamine biosynthetic pathway in cancer. BMC Biol. 2019;17:52.
15. Fang B, Miller MW. Use of galactosyltransferase to assess the biological function of O-linked N-acetyl-d-glucosamine: a potential role for O-GlcNAc during cell division. Exp Cell Res. 2001;263:243–53.
16. Wellen KE, Thompson CB. A two-way street: reciprocal regulation of metabolism and signalling. Nat Rev Mol Cell Biol. 2012;13:270–6.
17. Chatham JC, Marchase RB. Protein O-GlcNAcylation: a critical regulator of the cellular response to stress. Curr Signal Transduct Ther. 2010;5:49–59.
18. Liu C, Li J. O-GlcNAc: a sweetheart of the cell cycle and DNA damage response. Front Endocrinol. 2018;9:415.
19. Munkley J. The glycosylation landscape of pancreatic cancer. Oncol Lett. 2019;17:2569–75.
20. Paiotta A, D'Orazio G, Palorini R, Ricciardiello F, Zoia L, Votta G, et al. Design, synthesis, and preliminary biological evaluation of GlcNAc-6P analogues for the modulation of phosphoacetylglucosamine mutase 1 (AGM1/PGM3). Eur JOC. 2018;2018:1946–52.

21. Ricciardiello F, Votta G, Palorini R, Raccagni I, Brunelli L, Paiotta A, et al. Inhibition of the hexosamine biosynthetic pathway by targeting PGM3 causes breast cancer growth arrest and apoptosis. Cell Death Dis. 2018;9:377.
22. Rodrigues JG, Balmana M, Macedo JA, Pocas J, Fernandes A, de-Freitas-Junior JCM, et al. Glycosylation in cancer: selected roles in tumour progression, immune modulation and metastasis. Cell Immunol. 2018;333:46–57.
23. Abbruzzese JL, Grunewald R, Weeks EA, Gravel D, Adams T, Nowak B, et al. A phase I clinical, plasma, and cellular pharmacology study of gemcitabine. J Clin Oncol. 1991;9:491–8.
24. Avril T, Vauleon E, Chevet E. Endoplasmic reticulum stress signaling and chemotherapy resistance in solid cancers. Oncogenesis. 2017;6:e373.
25. Palam LR, Gore J, Craven KE, Wilson JL, Korc M. Integrated stress response is critical for gemcitabine resistance in pancreatic ductal adenocarcinoma. Cell Death Dis. 2015;6:e1913.
26. Zinszner H, Kuroda M, Wang X, Batchvarova N, Lightfoot RT, Remotti H, et al. CHOP is implicated in programmed cell death in response to impaired function of the endoplasmic reticulum. Genes Dev. 1998;12:982–95.
27. Ardito CM, Gruner BM, Takeuchi KK, Lubeseder-Martellato C, Teichmann N, Mazur PK, et al. EGF receptor is required for KRAS-induced pancreatic tumorigenesis. Cancer Cell. 2012;22:304–17.
28. Liu YC, Yen HY, Chen CY, Chen CH, Cheng PF, Juan YH, et al. Sialylation and fucosylation of epidermal growth factor receptor suppress its dimerization and activation in lung cancer cells. Proc Natl Acad Sci USA. 2011;108:11332–7.
29. Lopez-Sambrooks C, Shrimal S, Khodier C, Flaherty DP, Rinis N, Charest JC, et al. Oligosaccharyltransferase inhibition induces senescence in RTK-driven tumor cells. Nat Chem Biol. 2016;12:1023–30.
30. Qian W, Li J, Chen K, Jiang Z, Cheng L, Zhou C, et al. Metformin suppresses tumor angiogenesis and enhances the chemosensitivity of gemcitabine in a genetically engineered mouse model of pancreatic cancer. Life Sci. 2018;208:253–61.
31. Olive KP, Jacobetz MA, Davidson CJ, Gopinathan A, McIntyre D, Honess D, et al. Inhibition of Hedgehog signaling enhances delivery of chemotherapy in a mouse model of pancreatic cancer. Science. 2009;324:1457–61.
32. Feng M, Xiong G, Cao Z, Yang G, Zheng S, Qiu J, et al. LAT2 regulates glutamine-dependent mTOR activation to promote glycolysis and chemoresistance in pancreatic cancer. J Exp Clin Cancer Res. 2018;37:274.
33. Uhlen M, Zhang C, Lee S, Sjostedt E, Fagerberg L, Bidkhori G. et al. A pathology atlas of the human cancer transcriptome. Science. 2017;357:eaan2507.
34. Itkonen HM, Minner S, Guldvik IJ, Sandmann MJ, Tsourlakis MC, Berge V, et al. O-GlcNAc transferase integrates metabolic pathways to regulate the stability of c-MYC in human prostate cancer cells. Cancer Res. 2013;73:5277–87.
35. Ma Z, Vocadlo DJ, Vosseller K. Hyper-O-GlcNAcylation is anti-apoptotic and maintains constitutive NF-kappaB activity in pancreatic cancer cells. J Biol Chem. 2013;288:15121–30.
36. Olivier-Van Stichelen S, Guinez C, Mir AM, Perez-Cervera Y, Liu C, Michalski JC, et al. The hexosamine biosynthetic pathway and O-GlcNAcylation drive the expression of beta-catenin and cell proliferation. Am J Physiol Endocrinol Metab. 2012;302:E417–24.
37. de Queiroz RM, Oliveira IA, Piva B, Bouchuid Catao F, da Costa Rodrigues B, da Costa, et al. Hexosamine biosynthetic pathway and glycosylation regulate cell migration in melanoma cells. Front Oncol. 2019;9:116.
38. Namba T, Kodama R. Avarol induces apoptosis in pancreatic ductal adenocarcinoma cells by activating PERK-eIF2alpha-CHOP signaling. Mar Drugs. 2015;13:2376–89.
39. Dauer P, Sharma NS, Gupta VK, Nomura A, Dudeja V, Saluja A, et al. GRP78-mediated antioxidant response and ABC transporter activity confers chemoresistance to pancreatic cancer cells. Mol Oncol. 2018;12:1498–512.
40. Thakur PC, Miller-Ocuin JL, Nguyen K, Matsuda R, Singhi AD, Zeh HJ, et al. Inhibition of endoplasmic-reticulum-stress-mediated autophagy enhances the effectiveness of chemotherapeutics on pancreatic cancer. J Transl Med. 2018;16:190.
41. Nagaraj NS, Washington MK, Merchant NB. Combined blockade of Src kinase and epidermal growth factor receptor with gemcitabine overcomes STAT3-mediated resistance of inhibition of pancreatic tumor growth. Clin Cancer Res. 2011;17:483–93.
42. Gao H, Korn JM, Ferretti S, Monahan JE, Wang Y, Singh M, et al. High-throughput screening using patient-derived tumor xenografts to predict clinical trial drug response. Nat Med. 2015;21:1318–25.
43. Liu X, Ory V, Chapman S, Yuan H, Albanese C, Kallakury B, et al. ROCK inhibitor and feeder cells induce the conditional reprogramming of epithelial cells. Am J Pathol. 2012;180:599–607.
44. Yang G, Wang H, Feng M, You L, Zheng L, Zhang T, et al. Integrated analysis of gene expression and methylation profiles of novel pancreatic cancer cell lines with highly metastatic activity. Sci China Life Sci. 2019;62:791–806.
45. Du Y, Liu Z, You L, Hou P, Ren X, Jiao T, et al. Pancreatic cancer progression relies upon mutant p53-induced oncogenic signaling mediated by NOP14. Cancer Res. 2017;77:2661–73.